CEFC2008 CD.PDF - Adobe Acrobat Pro

파일(F) 편집(E) 보기(V) 문서(D) 주석(C) 양식(R) 도구(T) 고급(A) 창(W) 도움말(H)

작성 결합 공동 작업 보안 서명 양식 멀티미디어 주석

a 1/680 78.1% 찾기

13TH IEEE CEFC 2008

Athens, 11-15 May 2008

Booklet

Program

Digests

Authors' Index by Page

Authors' Index by Session

Search

PD5-8 **Finite Element Based Estimator for High-Performance Switched Reluctance Machine Drives** 373
Iakovos St. Manolas, Antonios G. Kladas
NATIONAL TECHNICAL UNIVERSITY OF ATHENS, GREECE

PD5-9 **Thermal Analysis of Magnetic Shields for Induction Heating** 374
Peter Sergeant[1], Dietrich Hectors[2], Luc Dupre[1], Koen Van Reusel[2]
[1]GHENT UNIVERSITY, BELGIUM, [2]KU LEUVEN, BELGIUM

PD5-10 **About Numerical Analysis Techniques for Solving the Coupled Electromagnetic and Thermal Field Question into Industrial Equipment with Moving Parts** 375
Teodor Leuca, Mircea N. Arion, Gabriel R. Cheregi
UNIVERSITY OF ORADEA, ROMANIA

PD5-11 **Multigrid Method for the Coupled Equation in Electromagnetic Centrifugal Casting** 376
Jinming Wang[1,2], Dongyang Wu[1], Dexin Xie[1]
[1]SHENYANG UNIVERSITY OF TECHNOLOGY, P.R. CHINA, [2]DALIAN UNIVERSITY OF TECHNOLOGY, P.R. CHINA

Invited Lecture MACEDONIA

15:40 – 16:10 Session Chair: **S. Hoole, A. Arkadan**

ID **Evolutionary Multiobjective Optimization Methods for the Shape Design of Industrial Electromagnetic Devices** 377
Paolo Di Barba
UNIVERSITY OF PAVIA, ITALY

OD1 – Material Modeling MACEDONIA

16:15 – 17:35 Session Chair: **E. Della Torre, D. Ioan**

OD1-1 **Evaluation of Hysteresis Losses in Iron Sheets Under DC-Biased Inductions** 378
C. Simão, N. Sadowski, N. J. Batistela, J. P. A. Bastos
GRUCAD/EEL/CTC/UFSC, BRAZIL

OD1-2 **An Improved Modeling of Vector Magnetic Properties of Electrical Steel Sheet for FEM Application and Its Experimental Verification** 379
Yanli Zhang[1], Young Hwan Eum[2], Wei Li[1], Dexin Xie[1], Chang Seop Koh[2]
[1]SHENYANG UNIVERSITY OF TECHNOLOGY, P.R. CHINA, [2]CHUNGBUK NATIONAL UNIVERSITY, KOREA

OD1-3 **A Novel Approach to Characteristic Analysis Considering Anisotropic Electrical Steel Sheets for Electrical Machines** 380
Soon-O Kwon[1], Jung-Jong Lee[1], Kyung-Ho Ha[2], Jung-Pyo Hong[1]
[1]HANYANG UNIVERSITY, KOREA , [2]POSCO, KOREA

OD1-4 **Numerical Identification Procedure for a Phenomenological Vector Hysteresis Model** 381
P. Burrascano[1], E. Cardelli[1], A. Faba[1], M. Ricci[1], A. Pirani[1], Edward Della Torre[2]
[1]PERUGIA UNIVERSITY, ITALY, [2]GEORGE WASHINGTON UNIVERSITY, USA

A Novel Approach to Characteristic Analysis Considering Anisotropic Electrical Steel Sheets for Electrical Machines

Soon-O Kwon[1], Jung-Jong Lee[1], Kyung-Ho Ha[2], and Jung-Pyo Hong[1], *Member, IEEE*

[1]School of Mechanical Engineering, Hanyang University, Seoul, 133-791, Korea
[2]Electrical Steel Research Group, Technical Research Lab., POSCO, Korea

This paper deals with characteristics analysis of Interior Permanent Magnet (IPM) motor considering anisotropy of electrical steel sheets. B-H data for various magnetization angle reference to rolling direction are measured and used for Finite Element Analysis (FEA) then, motor characteristics of core loss, back Electro-Motive Force (EMF), and cogging torque are calculated. An IPM motor is analyzed considering isotropy and anisotropy. Results of isotropy and anisotropy analysis are compared and verified by experiments.

***Index Terms*— Finite element analysis, Permanent magnet motors, Magnetic materials**

I. Introduction

Finite Element Analysis (FEA) is generally used for the analysis and design of electrical machines. To improve its accuracy, more precise material data should be provided. Electrical steel sheets are classified into isotropic and anisotropic, and isotropic steel sheets are generally used for electrical motors and anisotropic steel sheets are used for transformer. Actually, isotropic steel have anisotropic B-H and core loss characteristics reference to rolling direction and the average value of rolling and transversal direction is provided by manufacturer. Therefore, using average characteristics of electrical steel sheets leads to difference between experimental and FEA results. Measurement and analysis method considering anisotropic material characteristics are researched [1], however, it requires complex technique in measurements and large computation time solving governing equation for FEA. Therefore this paper presents simple but clear test method for anisotropic electric steel core and analysis method considering anisotropic materials. Simple test for measuring core loss and B-H data for anisotropic materials and FEA analysis using measured data are presented.

For the verification of analysis, an IPM motor is fabricated and tested. Permanent magnet motors have higher power density than other type motor of induction motor, switched reluctance motors, etc. Especially IPM type synchronous motors utilize both magnetic and reluctance torque, they have higher power density than surface permanent magnet motor and this leads to growing interests for wide applications. Therefore many IPM type motors are designed and sometimes significant difference of motor parameter occurs between experiment and FEA result [2].

II. Measurement of B-H and Core Loss Data

B-H and core losses are measured by Single Sheet Test (SST) reference to the angle from rolling direction and results are shown in Fig. 1, and angle is defined from rolling direction in the figure. In Fig. 1 it is shown that the lowest B-H characteristics occurs about 45º. Therefore, it is expected that the average B-H data of rolling and cross rolling direction will results in difference between analysis and experiments. Fig. 2 presents specimen for SST, and 7 specimens are cut and the size is 150×150 mm.

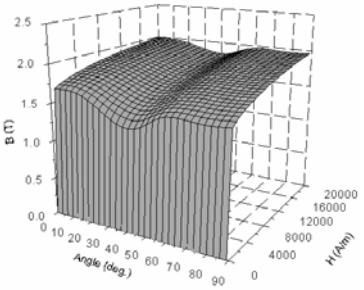

Fig. 1. Measured B-H data according to angle from rolling direction.

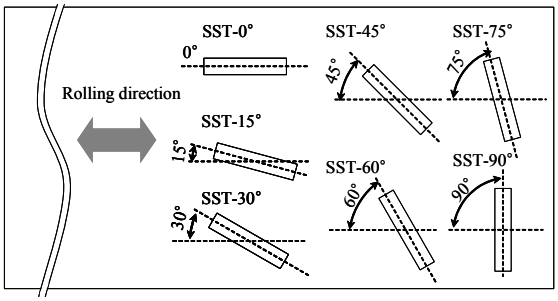

Fig. 2. Cutting of specimens for SST.

III. Analysis Method and Procedure

A. Analysis process

Measured B-H data are interpolated and prepared for 2-dimensional FEA. B-H data consist of B, H, and θ (angle from rolling direction). Using B-H data, FEA is conducted then core loss is calculated [2]. Solving procedure of FEA is shown in Fig. 3. As shown in Fig. 3, governing equation is solved with the initial permeability of material then flux density and θ are calculated in each element. With the flux density and θ, new permeability is found from B-H data then governing equation is calculated again until the error is converged.

Digital Object Identifier inserted by IEEE

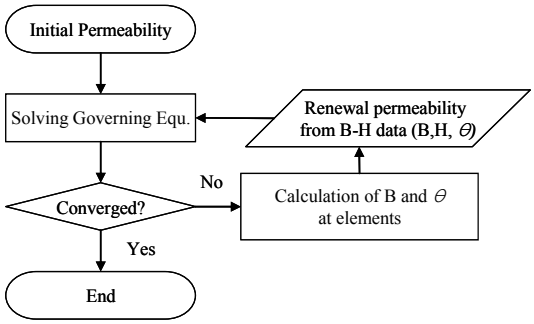

Fig. 3. FEA process.

IV. FEA RESULTS AND VERIFICATIONS

A. Analysis Model

Table I. shows the major motor dimensions and parameters. The analysis model has 4-poles and 6-slots with concentrated windings and shown in Fig. 4, and fabricated rotor core and completed view is shown in Fig. 5. The model has 2mm of bridge width for the study of the effect of bridge width, and thick bridge can be seen Fig. 5(a).

TABLE I
MAJOR DIMENSIONS AND PARAMETERS

Number of poles	4
Stator outer radius (mm)	117
Stator inner radius(mm)	47.4
Airgap length(mm)	0.7
Rotor outer radius(mm)	46
Stack Length(mm)	45
Magnet remanent flux density(T)	1.2
Magnet recoil permeability	1.05
Stator and rotor core material	50PN595

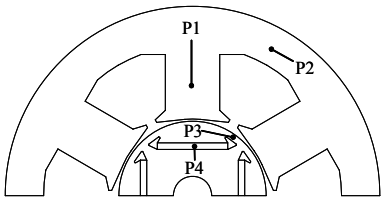

Fig. 4. Rotor and stator structure (1/2 model), and P1~P4 represents the position of elements to estimate flux densities and core loss densities.

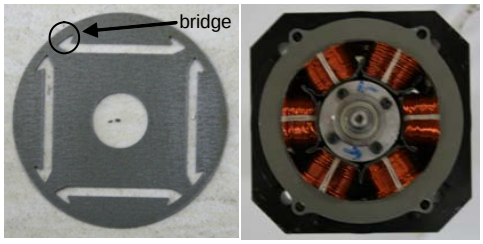

(a) Rotor core. (b) Assembled motor.

Fig. 5. Top view of fabricated rotor core and assembled motor.

B. B-H data for High H Field

B-H data provided by steel manufacturer are limited due to practical reason. In the IPM type motor, flux density in bridge region is generally beyond provided material data. Therefore, flux density should be modeled according to field intensity. For the isotropy analysis, flux density is calculated with relative permeability of air for the increase of field intensity. For the anisotropic analysis, last slope of measured data is maintained.

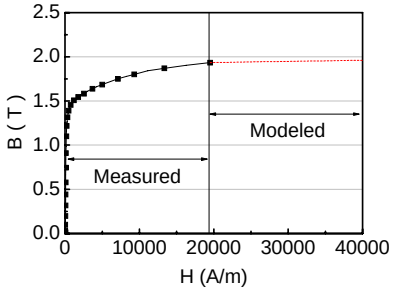

Fig. 6. B-H data modeling

C. Flux densities at no load

Fig. 8 shows the flux density variation at no load according to rotor positions of P1 ~ P4 shown in Fig. 4. In the comparison, only main flux density components in each part are presented. For the tooth (P1) and yoke part (P2), Isotropy analysis results show higher flux density in fundamental component.

In the bridge part (P3), higher tangential flux density is observed with anisotropy analysis and also higher core loss is expected due to magnitude and harmonics.

In the permanent magnet part (P4), higher eddy current loss in permanent magnet is expected when anisotropy is considered due to higher harmonics and fundamental component flux density. Even though higher operating point of permanent magnet, higher leakage flux through bridge part leads to decreased linkage flux.

D. No load back EMF

No load back EMF is the major motor parameters and should be expected precisely. However, differences between FEA and experiments occur sometimes and this leads to change of the entire motor characteristics.

No load line to line back EMF comparisons are shown in Fig. 7. There is significant difference between experiment and isotropy analysis; 11% higher back EMF than experiment. This difference affects to the entire motor performance, such as efficiency, rated current, voltage, etc. By considering anisotropy of core material, back EMF is precisely calculated; 1.9% higher than experiment.

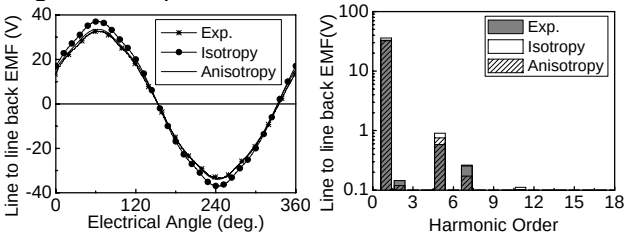

Fig. 7. Comparison of line to line no load back EMF at 25°C and 1000rpm.

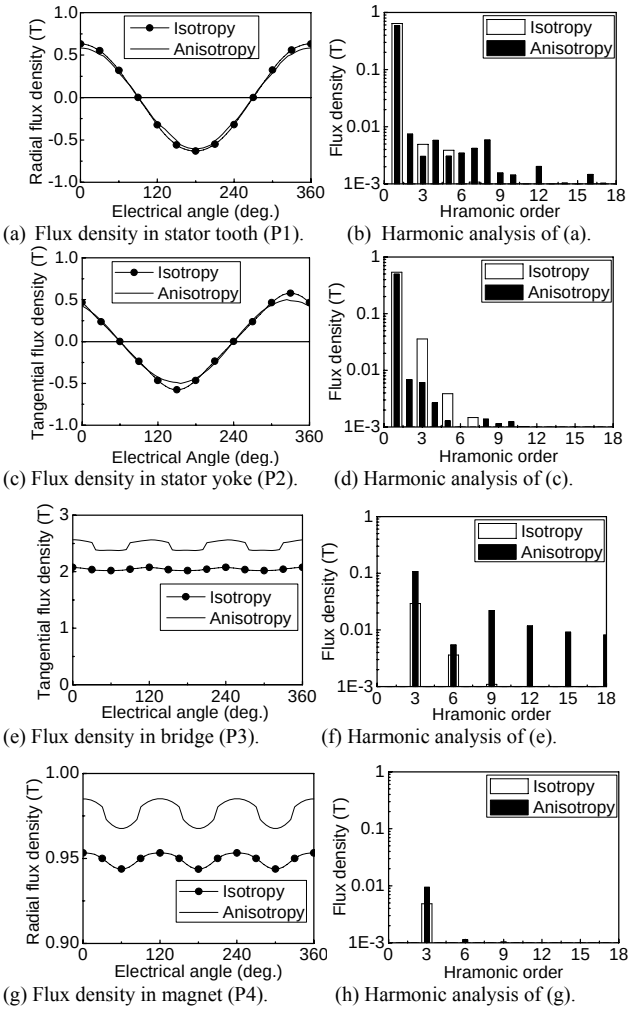

(a) Flux density in stator tooth (P1). (b) Harmonic analysis of (a).

(c) Flux density in stator yoke (P2). (d) Harmonic analysis of (c).

(e) Flux density in bridge (P3). (f) Harmonic analysis of (e).

(g) Flux density in magnet (P4). (h) Harmonic analysis of (g).

Fig.8. Flux density and harmonic analysis at P1~P4 in Fig. 4.

E. *Core loss and cogging torque*

Core losses are calculated by FEA based on measured core loss data [3]. No load core losses versus speed are shown in Fig.8, and there is small difference between two analysis results of the studied model. For the separation of core loss from mechanical loss in the experiment, a rotor with non-magnetized permanent magnet is additionally fabricated for mechanical loss measurement.

Fig. 9 shows the cogging torque comparison, the peak value can be acceptable for both analysis results. Measured cogging torque wave form is asymmetric positive and negative value, and this is shown well with anisotropy analysis.

Fig. 10 shows the core loss density distributions and Table II. shows core loss densities for P1~P3. There is no significant in the stator part, however, in bridge part higher core loss density is observed when anisotropy is considered. Higher core loss density leads to higher local heating in bridge area, and this result in weakening of mechanical strength of bridge area. For the magnetic design aspect of IPM motor, bridge area are preferred to be as thinner as possible to reduce leakage flux of permanent magnet.

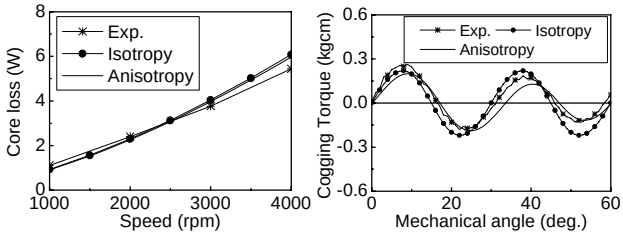

Fig. 8. Comparison of core loss Fig. 9. Comparison of cogging torque

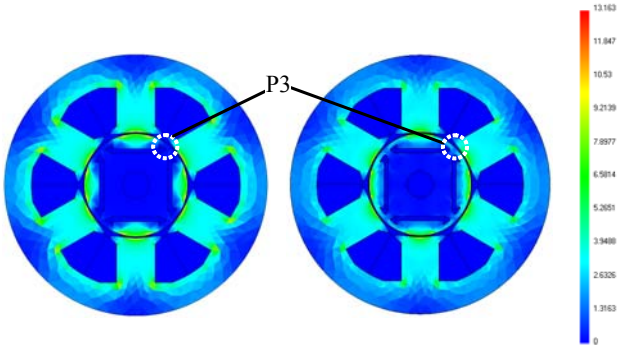

(a) Isotropy analysis (b) Anisotropy analysis

Fig. 10. Core loss density distribution.

TABLE II
CORE LOSS DENSITY COMPARISON AT P1~ P3 AT 25ºC, 4000RPM (W/KG)

Position	Isotropy	Anisotropy
Tooth (P1)	3.006	3.067
Yoke (P2)	2.263	2.070
Bridge (P3)	0.261	2.435

F. *Inductance*

Inductance is the major motor parameter with back EMF. Especially for the IPM type synchronous motor, d-axis inductance determines the characteristic current with no load flux linkage, therefore, determines the entire motor characteristics. There are a number of methods available to determine the inductances by FEA [4], [5]. Three phase flux linkage FE method is used for inductance calculation and its results are shown in Fig. 11 18% and 7% higher d-q axis inductances are estimated by anisotropy analysis.

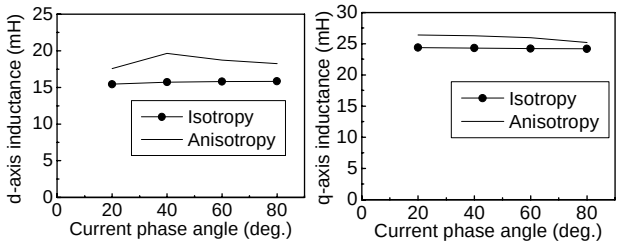

(a) d-axis inductance (b) q-axis inductance

Fig. 11. Comparison of d-q axis inductance (1Arms)

G. *Output Performance*

To compare output performances due to parameter differences, d-q axis equivalent circuit simulation is used and

parameters are shown in Table III. Linkage flux by permanent magnet (ψ_a), d- and q-axis inductances are calculated by FEA and core loss resistance is modeled considering rotating speed using core loss in Fig. 8 and ψ_a in Fig. 7 [7].

Output power and torque vs. speed of the motor are shown in Fig. 13. In order to get performance shown in Fig. 13, maximum torque per current and maximum efficiency control are applied to constant torque region and constant power region respectively. The simulation results are not necessarily precise at this point, and relative difference of performance is focused.

In the comparison of line to line voltage in Fig. 14, anisotropy simulation shows lower voltage increases due to lower back EMF. For the input current, due to lower linkage flux by permanent magnet, anisotropy simulation shows higher input current for required output torque in most operating region. Maximum current for anisotropy and isotropy simulation are 1.52 and 1.4Arms respectively. Maximum efficiency is found at 4000rpm in both analysis and 93% for anisotropy and 93.4% for isotropy analysis. In the low speed region, minimum efficiency of 79.5% for anisotropy and 81.8% for isotropy analysis are occurred.

TABLE III.
PARAMETERS FOR D-Q AXIS EQUIVALENT CIRCUIT ANALYSIS AT 75°C

	Isotropy	Anisotropy
Line to line voltage (Vrms)	100	100
Pole pair	2	2
Ψ_a(Wb)	0.09368	0.0857
d-axis inductance (mH)	Fig. 10(a)	Fig. 10(a)
q-axis inductance (mH)	Fig. 10(b)	Fig. 10(b)
Phase resistance (Ω)	1.28	1.28
Core loss resistance (Ω)	$3.23+24.93\omega_e^{0.63}$	$2.50+21.7\omega_e^{0.63}$

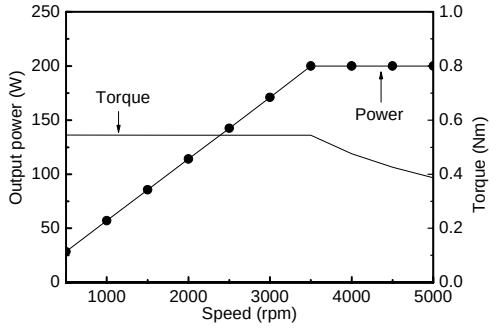

Fig. 13. Output torque and power-vs.-speed.

V. CONCLUSION

This paper has presented measurement of anisotropic core material and FEA considering anisotropy. Parameters of IPMSM are calculated and verified by experiments. It is found that the back EMF, inductance, and core loss distribution of IPMSM can be significantly different by considering anisotropy of material and this leads to the difference of output performances.

Presented approaches to estimate motor parameters can be a good reference for solving problems of differences between FEA and experiments. The differences between FEA and experiments in IPM type motor does not always take places due to anisotropy of material, and rotating lamination alleviate the effect of anisotropy.

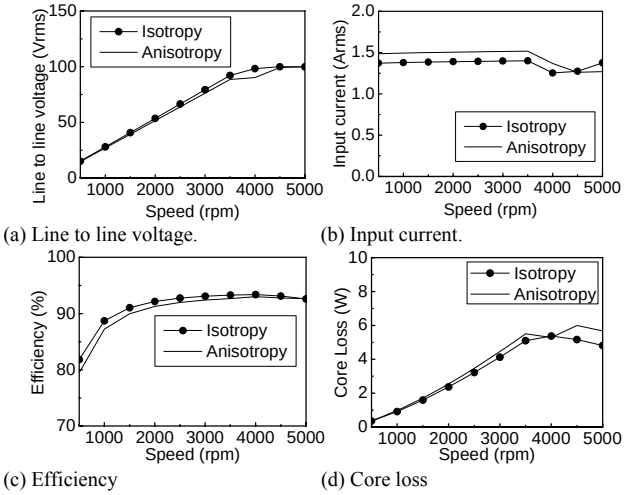

(a) Line to line voltage. (b) Input current.
(c) Efficiency (d) Core loss

Fig. 14. d-q axis equivalent circuit simulation results.

REFERENCES

[1] T. Nakata, N. Takahashi, K. Fujiwara and M. Nakano, ″Measurement of Magnetic Characteristics along Arbitrary Direction s of Grain-Oriented Silicon Steel Up to High Flux Densities″, *IEEE Trans. Magn.*, Vol. 29, No. 6, Nov. 1993.

[2] T. M. Jahns, S.H Han, A. M. EL-Refaie, J.H Baek, M. Aydin, M. K. Guven and W.L Soong, ″Design and experimental verification of a 50kW interior permanent magnet synchronous machine″, *IEEE Trans. Magn.*, Vol. 39, No. 3, May 2006.

[3] H. Nam, K. H Ha, J. P. Hong and G. H. Kang, ″A study on iron loss analysis method considering the harmonics of the flux density waveform using iron loss curves tested on Epstein samples″, *IEEE Trans. Magn.*, Vol. 39, No. 3, May 2003.

[4] J.Y Lee, S.H Lee, G.H. Lee, J.P. Hong, J.Hur, ″Determination of parameters considering magnetic nonlinearity in an interior permanent magnet synchronous motor″, *IEEE Trans. Magn.*, Vol. 42, No. 4, Apr. 2006.

[5] R. Dutta and M. F. Rahman, ″ A Comparative Analysis of Two Test Methods of Measuring d- and q-Axis Inductances of Interior Permanent –Magnet Machine ″, *IEEE Trans. Magn.*, Vol. 42, No. 11, Nov. 2006.

[6] S. Morimoto, H. Kato, M. Sanada, and Y. Takeda, ″Output Maximization Control for Wind Generation System with Interior Permanent Magnet Synchronous Generator″, *IEEE Trans. Magn.*, Vol. 42, No. 11, Nov. 2006.

Manuscript received March 3, 2008. Corresponding author: Jung-Pyo Hong (e-mail: hongjp@hanyang.ac.kr; phone: 82-2-2220-0455; Fax: 82-2-2220-4465).